ENVIRONMENTAL RESEARCH
LETTERS

LETTER • OPEN ACCESS

Community-scale changes to landfast ice along the coast of Alaska over 2000-2022

To cite this article: Sarah W Cooley and Jonathan C Ryan 2024 *Environ. Res. Lett.* **19** 024013

IOP Publishing Environ. Res. Lett. 19 (2024) 024013 https://doi.org/10.1088/1748-9326/ad1c7b

ENVIRONMENTAL RESEARCH
LETTERS

CrossMark

OPEN ACCESS

RECEIVED
13 October 2023

REVISED
24 December 2023

ACCEPTED FOR PUBLICATION
9 January 2024

PUBLISHED
19 January 2024

LETTER

Community-scale changes to landfast ice along the coast of Alaska over 2000-2022

Sarah W Cooley* **and Jonathan C Ryan**

Department of Geography, University of Oregon, Eugene, OR, United States of America
* Author to whom any correspondence should be addressed.

E-mail: scooley2@uoregon.edu

Keywords: Alaska, landfast ice, Arctic, climate change, remote sensing

Supplementary material for this article is available online

Abstract

Landfast sea ice that forms along the Arctic coastline is of great importance to coastal Alaskan communities. It provides a stable platform for transportation and traditional activities, protects the coastline from erosion, and serves as a critical habitat for marine mammals. Here we present a full assessment of landfast ice conditions across a continuous 7885 km length of the Alaska coastline over 2000–2022 using satellite imagery. We find that the maximum landfast ice extent, usually occurring in March, averaged 67 002 km^2 during our study period: equivalent to 4% of the state's land area. The maximum extent of landfast ice, however, exhibits considerable interannual variability, from a minimum of 29 871 km^2 in 2019 to a maximum of 87 571 km^2 in 2010. Likewise, the landfast ice edge position averages 22.9 km from the coastline but, at the community-scale, can range from 2.8 km (in Gambell) to 71.1 km (in Deering). Landfast ice breakup date averages 2 June but also varies considerably both between communities (3 May in Quinhagak to 24 July in Nuiqsut) and interannually. We identify a strong control of air temperature on breakup timing and use this relationship to project future losses of ice associated with Paris Climate Agreement targets. Under 2 °C of global air temperature warming, we estimate the average Alaskan coastal community will lose 19 days of ice, with the northernmost communities projected to lose 50 days or more. Overall, our results emphasize the highly localized nature of landfast ice processes and the vulnerability of coastal Arctic communities in a warming climate.

1. Introduction

The annual formation and breakup of landfast sea ice along the Arctic coastline is one of the most dramatic seasonal environmental changes anywhere on Earth. Unlike drift ice, which forms in the open ocean and drifts under wind and ocean currents, landfast ice is a stable platform attached to the coastline and/or grounded in shallow waters. Despite representing only ~12% of the global sea ice cover, landfast ice has outsized importance to the Arctic environment and ecosystems [1]. Landfast ice acts as a barrier between the ocean and the atmosphere, altering heat transfer and influencing local weather and ocean circulation patterns [2, 3]. In areas where the coast is subsiding, such as much of western Alaska, the presence of landfast ice can mitigate coastal erosion by dampening wave action during winter storms [4–6]. Ecologically, landfast ice is a critical habitat for ringed seals and polar bears, providing them with ideal denning locations [7] and the polynyas that form at the seaward landfast ice edge (SLIE) are areas of high ecological productivity. Indigenous Arctic communities have therefore relied upon landfast ice for subsistence hunting and fishing for thousands of years [8]. Whaling from the landfast ice edge is an activity of great cultural importance in many Arctic communities [9]. Given its stability and persistence, landfast ice also connects otherwise isolated communities given the absence of road networks in the region. This ability to travel from one community to another and access hunting grounds using landfast ice thus has significant economic, cultural and food security implications for people living in the Arctic [8, 10, 11].

Over the past ∼30 yr, Arctic residents have observed declines in the landfast ice surrounding their communities [10, 12–14]. Poor ice conditions increase the risk of winter travel and undermine earning opportunities and subsistence activities, particularly in areas where hunting and fishing are integral components of the local economy. Furthermore, communities have noted that well-known pan-Arctic declines in drift ice extent and concentration do not correlate well with local experiences of landfast sea ice [10]. Local Arctic residents have therefore consistently requested improved scientific understanding of landfast sea ice processes to enable them to safely use the ice and adequately plan for the future [8, 10, 11].

Researching landfast sea ice is challenging, since it requires imagery with sufficiently high spatial resolution to observe ice extent along complex coastal margins and sufficiently high temporal resolution to identify rapid fracture and breakup which can occur in days to weeks. Most scientific studies of landfast ice have therefore relied on synthetic aperture radar (SAR) to track changes in ice cover over local areas or short time periods [3, 15, 16]. However, these studies are limited by data availability as well as the challenge of distinguishing between melting ice and open water in SAR imagery. Other studies have used operational ice chart records to analyze long-term patterns in landfast ice [17–19]. These records are valuable but are generally only available ∼biweekly, too coarse for use at a community-scale, and contain their own biases related to data assimilation. A recent study presented a new approach for mapping landfast ice breakup at high spatial and temporal resolution using MODIS imagery [20]. However, their analysis only investigated breakup timing and focused on Northern Canada and Greenland where the presence of deep, narrow fjords and steep continental shelfs leads to different mechanisms of ice formation and breakup compared to the shallow shelves of Alaska. Notably, no work has analyzed decadal-scale changes along the entire ice-affected coast of Alaska, despite the significant threat many of these communities face due to the combined effects of coastal erosion and ice loss.

In this paper, we present a novel climatology of landfast sea ice in 38 Alaskan coastal communities over 2000–2022. We develop this dataset using a novel MODIS-derived method which allows us to map both the position of the SLIE and detect breakup timing at high spatial and temporal resolution. We then identify controls on both ice edge position and breakup timing by combining our dataset with climate reanalysis data and bathymetric data. We conclude by discussing projected future changes in landfast ice in Alaskan communities under different Paris Climate Agreement global temperature warming targets, namely 1 °C, 1.5 °C, and 2 °C.

2. Study area

We analyze landfast ice across 7885 km of Alaska's coastline, spanning from the coastal border with Canada on the Beaufort Sea to the mouth of the Egegik river at the head of the Alaska Peninsula (at approx. 58.1°N). Our study area also includes St. Lawrence Island and Nunivak Island. This broad region of coastal Alaska is experiencing some of the fastest warming on Earth [21] and is especially threatened by a combination of ice loss, increasing storm frequency, and enhanced coastal erosion [22–26]. Within this region, there are 38 coastal (or near-coastal) Alaskan communities on which we focus our analysis (figure 1). These communities have strong cultural ties to landfast ice, with many relying on the ice for subsistence activities such as hunting and whaling as well as for transportation [11, 27, 28]. The total population of these communities is 30 371, and the largest communities are Utqiagvik (4,927), Nome (3,699), and Kotzebue (3,102) [29].

3. Methods

Our novel landfast ice climatology is developed using NASA's MODIS sensor aboard the Terra satellite. Our climatology contains two key metrics relevant for communities in Alaska: landfast ice edge position and landfast ice breakup timing.

3.1. Ice edge position

We detect the position of the SLIE using a 30 day ice occurrence product derived from classified MODIS imagery. We first mask out land and identify non-cloud impacted pixels using MODIS's MOD09GA cloud mask product resampled to 250 m resolution. We then classify MODIS pixels in each daily image into ice or water using a 0.1 reflectance threshold in the MOD09GQ band 2 (near-infrared, 841–876 nm) surface reflectance product (following [20]). Ice occurrence is defined as (d = day):

$$\text{Ice Occurrence} = \frac{\sum_{d-30}^{d} \text{ice pixels}}{\sum_{d-30}^{d} \text{cloud - free pixels}}. \quad (1)$$

Ice occurrence therefore represents the percentage of time a pixel was classified as ice (vs. classified as water) over a 30 day period, accounting for the effect of cloud cover.

The SLIE is easily identified in the ice occurrence products by both a persistent, stable polynya which separates the landfast ice from drift ice and the smooth texture of the landfast ice surface (figure S1). We thus are able to delineate the SLIE position for each year manually using a stylus and a tablet (see SI). The annual maximum SLIE usually corresponds to ice presence during March and early April (i.e. the 30 day ice occurrence product is calculated over March 1st to April 1st or March 15th to April 15th; see SI). We

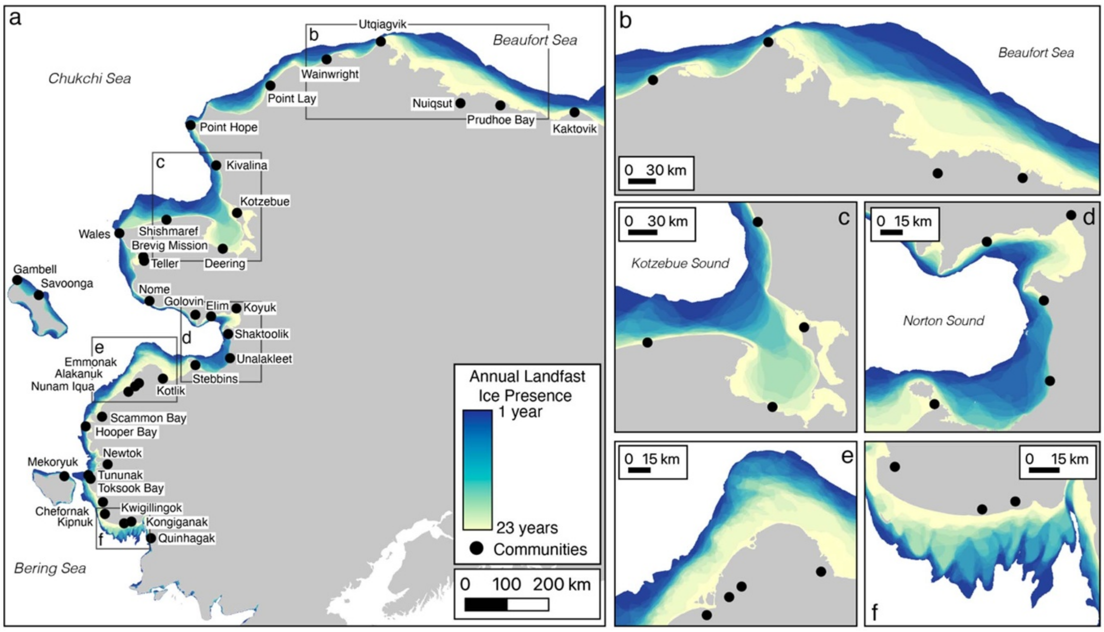

Figure 1. Annual landfast ice presence in Alaska over 2000–2022. Panel (a) shows our entire study region, with our focus 38 communities labeled. The colored fringe along the edge of the figure shows the frequency of landfast ice presence over our 23 yr record, with light yellow representing landfast ice present all years and dark blue showing areas covered by landfast ice in only one year. Panels (b) through (f) show ice edge position in greater detail in five regions of interest.

determine the mean distance of the ice edge from the coastline within 100 km of each community for each year by calculating the shortest distance to the SLIE for each approximately 350 m segment of coastline.

3.2. Breakup timing

We calculate breakup timing using the daily classified MODIS images described above. We first mask out all areas seaward of the landfast ice edge for each year. This step limits the influence of drift ice on breakup detection, since only areas contained within the maximum extent of landfast ice for each year are analyzed, and also accounts for interannual differences in landfast ice extent. Next, we produce a time series of percent water, calculated as # water pixels/(# water + # ice pixels) from the classified MODIS imagery within the annual landfast ice area.

We filter the time series by first removing observations where more than 75% of the landfast ice area is cloud-covered. We then apply a Hampel outlier filter and a 5 day median filter to remove spurious values. Breakup timing is identified by determining the first day the area within the landfast ice mask reaches 25%, 50%, 75% and 90% open water (figure S2). These dates are corrected for cloud cover by assigning the actual breakup date as the midpoint between the first date where the water percentage reaches this amount and the previous cloud-free observation. While there is no standard definition of breakup in the scientific literature, the rest of the paper focuses on the 75% open water threshold because it is arguably most relevant for Alaskan communities: by the time the coast is 75% water, it is likely that ice activities have ended and most open water activities have begun. We run this method for each of our communities for each year between 2000 and 2022.

3.3. Ancillary/driver analyses

We assess controls on spatial patterns in SLIE and breakup timing by deriving measures of bathymetry and mean annual air temperature for each community. Bathymetry is calculated by averaging the distance from the coastline to the 20 m contour in the GEBCO 2022 global gridded bathymetry dataset [30] (see SI). Mean annual air temperature is computed by averaging the 2 m (surface) air temperature product from ERA5 global atmospheric reanalysis [31, 32] (see SI).

Next, to better understand controls on interannual landfast ice variability, we use ERA5 air temperature data to assess the relationship between (1) winter (DJF) air temperature vs. SLIE and (2) spring air temperature vs. breakup timing. Given the substantial variability in the timing of ice breakup for each community, we define 'spring' as the 60 days prior to the 5 days before the earliest observed breakup for each community, meaning 'spring' is a different period for each community (following [20]). We specifically analyze temperature data over ice-covered seasons (hence ending our 'spring' period five days prior to the earliest breakup for each community) to ensure that changes in air temperature are driving the ice fluctuations, rather than ice extent fluctuations driving changes in air temperature through the ice albedo feedback. We also assess the relationship between drift ice and landfast ice edge position/breakup timing using the daily NSIDC sea ice concentration data record produced from passive microwave satellite observations [33]. To do this, we calculate the maximum annual drift ice concentration within 250 km of the community.

For all ancillary variable analyses (except sea ice), values are calculated as averages within 100 km of each community. Relationships between our independent (bathymetry, air temperature, drift ice concentration) and dependent (SLIE and breakup) variables are assessed using Pearson's R correlation tests for variables which are normally distributed (87% of all examined variables) and Spearman's correlation for non-normally distributed variables [34] (normality determined using the D'Agostino-Pearson test [35], see SI). We also test for trends in our edge position and breakup time series using the modified Mann-Kendall test for monotonic trend [36–38] which is commonly used for trend analysis in relevant sea ice literature ([39, 40] see SI).

3.4. Estimation of ice loss under different Paris Agreement scenarios

To project ice loss under different climate warming and mitigation scenarios, we combine our observed breakup sensitivities to springtime air temperature with an analysis of Arctic Amplification rates [21] and Paris Climate Agreement targets. The projected loss in ice days is calculated as follows:

$$\text{Ice Loss (days)} = \Delta T_{\text{PCA}}\,(^\circ\text{C}) * AA * \text{Sensitivity}\left(\frac{\text{days}}{^\circ\text{C}}\right) \quad (2)$$

where ΔT_{PCA} = the Paris Climate Agreement target for global mean temperature warming (i.e. 1 °C, 1.5 °C or 2 °C), AA = the Arctic Amplification rate, calculated for the 100 km surrounding each community using data from [21], and Sensitivity = the observed loss of ice days for each degree of temperature warming (days/°C), calculated for each community based on the linear relationship between springtime air temperature and breakup over our 23 yr record (see SI). We only estimate future ice loss for communities where springtime air temperature and breakup are correlated at $p < 0.05$.

4. Results

4.1. A climatology of Alaskan landfast ice

Over our 2000–2022 study period, we find that the landfast ice edge position (SLIE) generally increases with latitude, but there are exceptions, implying that local bathymetry and coastline complexity also play a role (figure 1). Over the entire ice-affected Alaskan coastline, mean SLIE distance from the coastline is 22.9 km (standard deviation = ±5.7 km), corresponding to a total average landfast ice area of 67 002 km^2. Across our 38 communities, mean SLIE ranged from a minimum of 2.8 km in Gambell (63.7°N) to 71.1 km in Deering (66.1°N) (figure 2, table S1). Broadly, communities in the Kotzebue Sound region and along the Beaufort Sea have the most extensive landfast ice, whereas the island communities and the southernmost communities along the Bering Sea have the least (figures 1 and 2). These overall patterns appear to be controlled by both bathymetry (defined by the distance to the 20 m contour, $R = 0.59$, $p < 0.001$) and broad-scale temperature gradients (mean annual air temperature, $R = -0.46$, $p < 0.01$) (figures 1, 2 and S5). In other words, we find the ice is more extensive where the shelf is shallower and the air temperature is colder.

The maximum ice extent occurred in 2010 and 2012: averaging 32.2 km from the coastline (87 471 km^2 of ice area in 2010; 86 271 km^2 in 2012) (figure 3). The minimum extent occurred in 2019 when the landfast ice edge only averaged 10.0 km from the coastline (29 871 km^2 of area). Temporally, we find the variability (defined as the standard deviation) in SLIE over our 23 yr record averages ±6.1 km, ranging from ±1.8 km in Mekoryuk to ±35.3 km in Deering. We do not observe a linear trend in Alaska-wide ice extent over our 23 yr record. Only one community (Kaktovik; $p = 0.005$) exhibits a statistically significant linear trend in SLIE decline. Therefore, ice extent has neither significantly increased nor decreased during our 23 yr study period, perhaps due to the large temporal variability in ice position we observe (figure 3).

We find that the mean breakup date across all communities is June 2nd (DOY 153) ±1.8 days due to clouds, ranging from Quinhagak (3 May ±2.2 d) to Prudhoe Bay and Nuiqsut (24 July ±1.2 and 2.1 days, respectively) (figure 2). The spatial patterns in mean breakup timing are almost entirely explained by mean annual air temperature ($R = -0.97$, $p < 0.0001$), with no statistically significant role of bathymetry (figures 2 and S5). Interannual breakup variability (defined by the standard deviation) averages 11.9 days, ranging from 8.7 days in Golovin to 16.4 days in Kaktovik. The latest average breakup occurred in 2000 (16 June), and the earliest average breakup occurred in 2018 (4 May). The time series of annual breakup timing, averaged across all communities, has a statistically significant trend towards earlier breakup over 2000–2022 (modified Mann-Kendall p value = 0.02), with a slope of −7.4 days/decade. Using the modified Mann-Kendall test, 14 communities have a trend significant at $p < 0.05$, and Kaktovik has the largest trend at −16.7 days/decade ($p < 0.001$).

Interestingly, we find that interannual variability in breakup timing is not necessarily correlated with ice edge position, particularly for the more northern communities (figure 4(c)). Only 14 out of 38 communities have significant correlations at $p < 0.05$, predominantly in the southern portion of

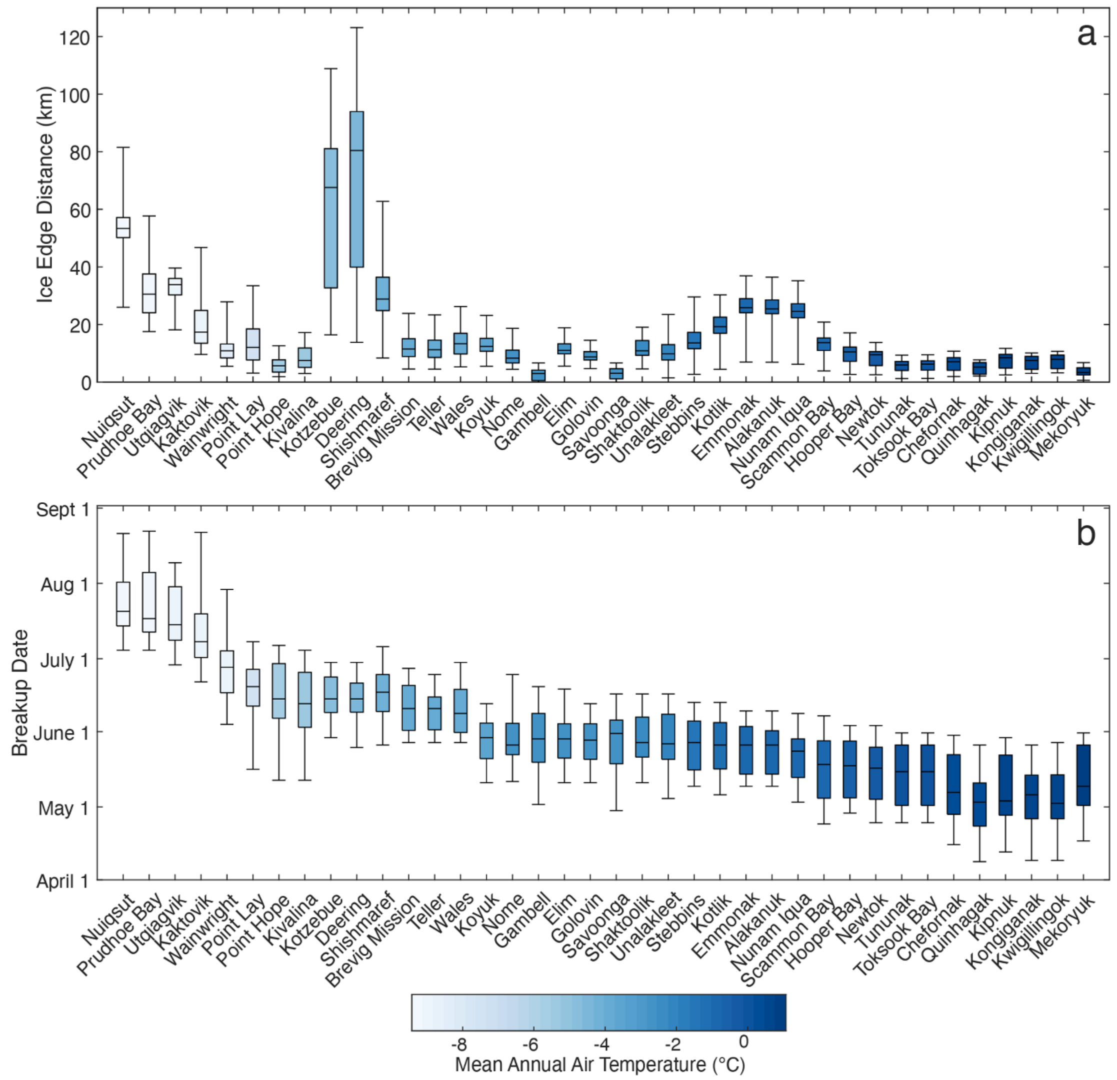

Figure 2. Annual ice edge position (a) and breakup date (b) by community, averaged over 2000–2022. Communities are ordered from coldest to warmest, with the color of the panel corresponding to each community's mean annual air temperature. The box edges display the interquartile range and the center line displays the median.

our study region. Therefore, for most communities, the formation of very extensive landfast ice in March does not necessarily mean that the ice will persist later into the summer.

4.2. Drivers of landfast ice variability

We find that 25 of 38 communities exhibit a statistically significant negative correlation between SLIE and winter air temperature at $p < 0.05$ (figures 4(a) and S3). The strongest correlations are found in the southernmost communities, with no correlations observed along the Chukchi and Beaufort Seas (figure 4(a)). We do not observe any notable patterns in SLIE sensitivity to winter air temperature (i.e. change in SLIE per change in winter temperature; km/°C), other than the sensitivities are broadly correlated with bathymetry (table S2, figure S6).

We identify strong correlations between spring air temperature and breakup timing across nearly the entire study region, finding 34 of 38 communities exhibit correlations at $p < 0.05$ (figures 4(b) and S4). Notably, we find that breakup timing in colder communities is more sensitive to air temperature ($R^2 = 0.58$, $p < 0.0001$; Figure S6), corroborating the findings of [20] in Canada and Greenland. The average sensitivity to air temperature is −3.6 days/°C, with the highest sensitivities found in the northernmost/coldest communities (Prudhoe Bay: −9.1 days/°C, Utqiagvik: −6.4 days/°C), and lowest sensitivities found in the southernmost/warmest communities (−2.0 days/°C in Kongigak and Quinhagak) (table S2). Finally, we find that the maximum drift ice concentration is correlated with both ice edge position in 27 of 38 communities and with breakup timing in 30 of 38, at $p < 0.05$ (figures 4(d) and (e); Table S2), with the strongest correlations found in the southernmost communities.

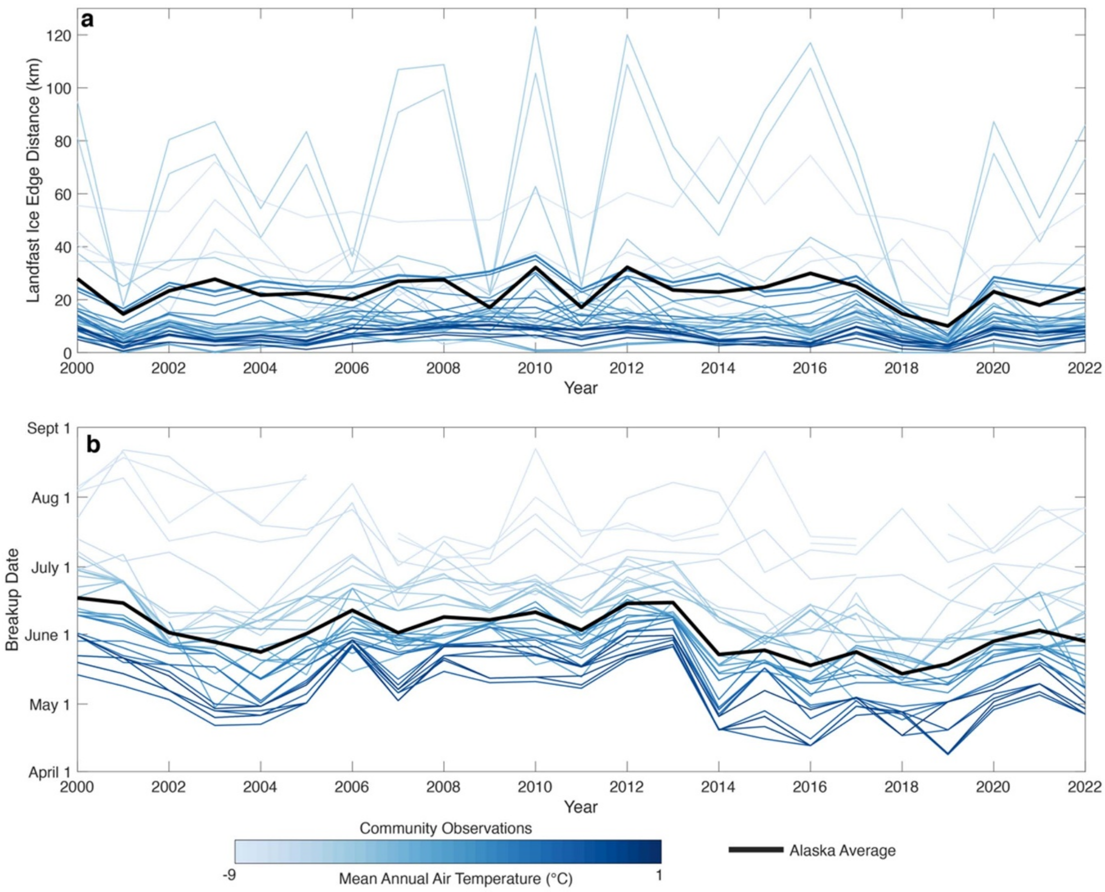

Figure 3. Time series of landfast ice edge distance (a) and breakup date (b) over 2000–2022 for each community. The Alaska average is shown in black, and the lines are colored by mean annual air temperature, with lighter colors representing colder communities. Gaps in the time series are due to missing observations and/or years where breakup could not be detected.

4.3. Projected loss of ice under different Paris Climate Agreement targets

By combining our observed sensitivities with Arctic Amplification rates, we estimate a projected loss of ice across Alaska of 9.5 days per 1 °C of global warming above pre-industrial levels, 14.2 days at 1.5 °C and 18.9 days at 2 °C (figure 5). However, these mean values mask substantial variability within Alaska. Since the northernmost and coldest communities experience greater warming and have more sensitive breakup to changes in air temperature (figure S6), the differences in projected ice loss are much greater than in the southernmost communities. For example, Utqiagvik is estimated to lose 52 days of ice at 2 °C of global warming, whereas the three southernmost communities (Kipnuk, Kwigillingok and Quinhagak) are estimated to lose only 7–8 days.

5. Discussion

Our study represents the first Alaska-wide assessment of landfast ice conditions, providing valuable insight into how these patterns vary across the region. Notably, we identify considerable interannual variability in SLIE during our study period. Across Alaska, the total landfast ice area variability ranged by 86% around the mean (from a minimum of 29 871 km^2 to a maximum of 87 571 km^2) but, in individual communities, that variability can be far greater. In Deering, the SLIE averaged 123 km from the coastline in 2010, whereas in 2019, the SLIE only extended 14 km from the coastline. This contrast in ice conditions from year to year has substantial impacts on communities. For example, in Nome, the landfast sea ice was so extensive in 2012 that an emergency wintertime delivery of fuel required transferring fuel via very long hoses which traversed atop the landfast ice [16]. Conversely, the anomalously low ice period of 2018–2019 in the Kotzebue Sound region reduced opportunities for subsistence hunting [11, 28].

Determining the drivers of this strong interannual variability in SLIE is challenging. Winter air temperature clearly exerts some control (25 of 38 communities are correlated at $p < 0.05$), but the lack of broadly consistent strong correlations indicates that other factors not considered in our analysis may influence ice edge position. However, we note that these other factors, which include ocean temperatures, currents, and wind speed/direction, are much harder to accurately simulate in climate reanalysis products compared with air temperatures [32, 41]. This lack of correlations as well as the enormous

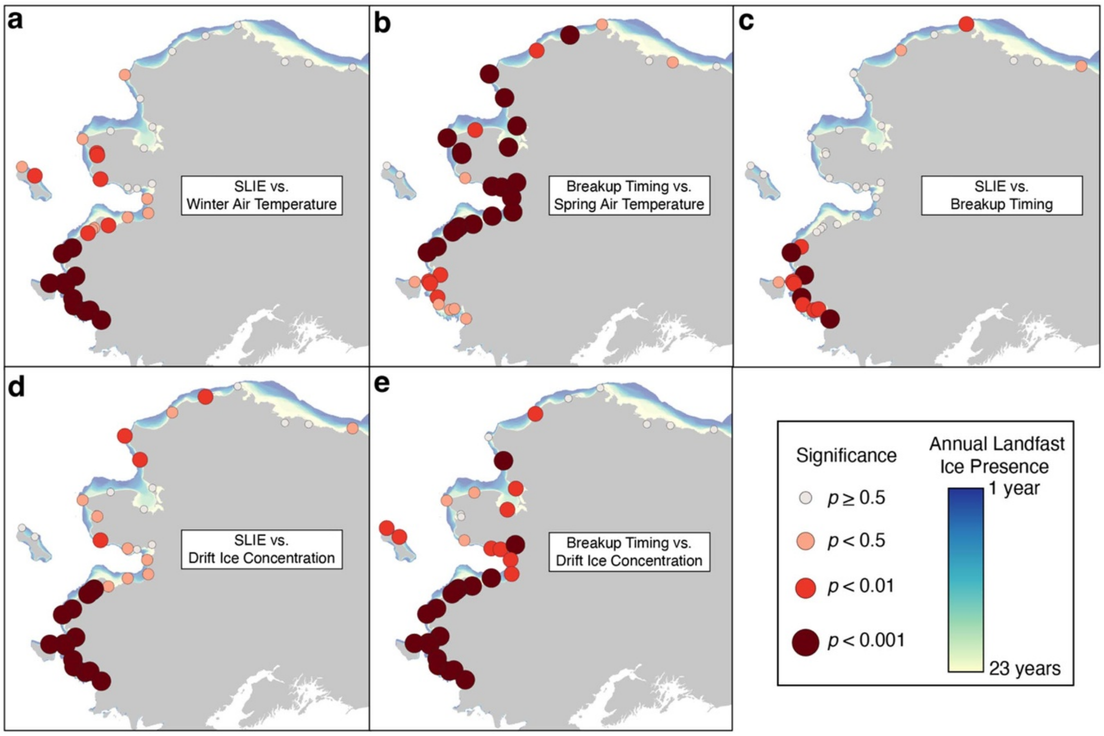

Figure 4. Correlation maps showing the relationship between different variables for each community. Each panel shows the p value for the correlation between SLIE (seaward landfast ice edge) distance from coastline and winter (DJF) air temperature (a), breakup timing and spring air temperature (b), SLIE and breakup timing (c), SLIE and drift ice concentration (d) and breakup timing and drift ice concentration (e). Relationships not significant at $p < 0.05$ are shown in light gray.

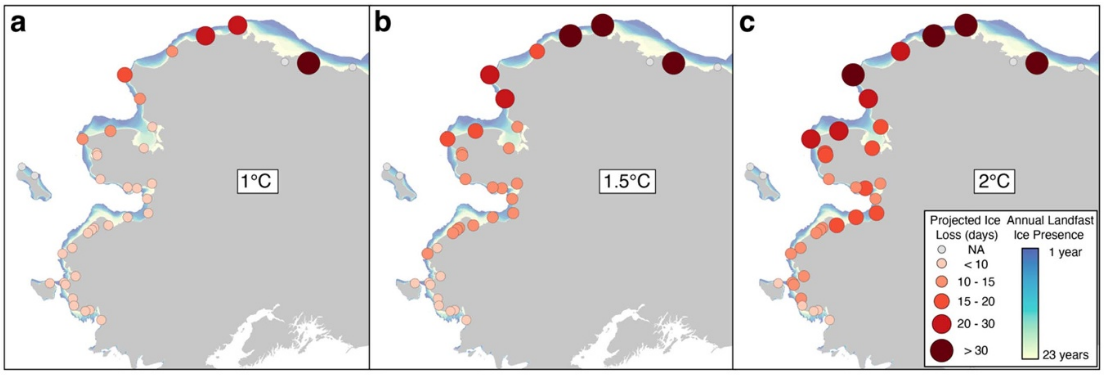

Figure 5. Projected loss of ice days due to earlier landfast ice breakup under different Paris Climate Agreement global temperature warming targets, namely 1 °C (a), 1.5 °C (b) and 2 °C (c).

year-to-year variability in ice extent make it difficult to predict future changes in ice extent, threatening safe ice travel and inhibiting adaptation for diminished future ice presence [11, 27]. It is also possible that the lack of significant correlations may be, at least partly, attributed to the limitations of our landfast ice detection method (see SI for additional discussion). While differences in texture and the presence of the ice edge polynya enable distinction between landfast ice and drift ice in our MODIS-derived ice occurrence product (figure S1), we cannot determine absolutely whether the landfast ice is 'stable' and grounded from the optical imagery alone. Therefore, our analysis may not necessarily represent all the ice that is accessible to community ice users. Future work identifying drivers of interannual variability in SLIE should thus consider incorporating additional field data such as in situ ice mass balance buoys as well as combining satellite data with local perspectives.

Interestingly, our analysis reveals a contrast between landfast ice conditions and processes in northern Alaska (along the Beaufort and Chukchi Seas) vs. central/southern Alaska (along the Bering Sea). In northern Alaska, ice is much more extensive (SLIE = 27.2 km vs. 10.8 km, on average), and breaks up later (25 June vs. 20 May), yet it is also more variable and the controls on its formation and breakup are more complex. Along the Beaufort and Chukchi

Seas, SLIE is generally uncorrelated with winter air temperature, years with more extensive ice do not necessarily tend to breakup earlier, and landfast ice formation and breakup appear to be independent of drift ice conditions. A potential reason for this may be that in the Bering Sea, there is a strong coupling between atmospheric and oceanic temperatures and sea ice formation that operates at a local- to regional-scale [42, 43]. In other words, years with a lower drift ice concentration and warmer temperatures in the Bering Sea are associated with increased energy exchange between the ocean and the atmosphere via the ice albedo feedback, leading to less extensive landfast ice and earlier breakup. In contrast, landfast ice extent in the Beaufort Sea is driven not only by local winter air temperatures but also by more distal factors such as Arctic Ocean wind patterns and Bering Strait inflow currents, which dilute the influence of local winter air temperatures [2]. This difficulty in identifying local controls on landfast ice formation along the Beaufort and Chukchi Seas emphasizes that northern communities face far greater challenges in predictability of ice conditions and future ice loss.

Although controls on ice edge position variability are complex, our results demonstrate that interannual patterns of breakup timing are well-predicted by spring air temperatures throughout Alaska, including in most communities along the Beaufort and Chukchi Seas. This finding highlights the fact that ice breakup is largely a thermal process driven by atmospheric interactions [28, 44] and corroborates previous research from elsewhere in the Arctic [20]. By using these strong relationships between breakup timing and spring air temperature to produce estimates of projected ice loss under different Paris Climate Agreement targets, we find Alaskan coastal communities will experience breakup 9.5 days earlier at 1 °C, 14.2 days earlier at 1.5 °C and 18.9 days earlier at 2 °C, with far greater losses (up to 62 days at +2 °C) expected in the northernmost communities. While the differences between these scenarios may appear small, they are likely to have substantial effects on the economy and livelihoods of many Alaskans. A longer open water season means the coastline will be more exposed to storms and waves, increasing the propensity for coastal erosion which already threatens many of these communities [6], especially those facing the real possibility of relocation [45]. A decrease in the duration of the ice season can also negatively impact food security [11]. In the more northern communities, whaling along the landfast ice edge is an important cultural activity that will also be impacted by large decreases in the length of the ice season as well as a declining ice extent [9, 46].

6. Conclusions

Our results present the first full assessment of landfast ice position and breakup timing across all of Alaska over 2000–2022. Landfast ice is extensive across much of coastal Alaska: equivalent to, on average, 4% of Alaska's land area. We find that landfast ice extent is both highly localized and highly spatially and interannually variable, whereas landfast ice breakup more neatly follows air temperature patterns. Our estimated ice loss under different Paris Climate Agreement targets emphasizes the sensitivity of ice breakup to even small changes in global average temperatures. The difference between 1.5 °C and 2 °C of warming can be difficult to communicate to the public, but translating these values to loss of ice days is likely to be much more relevant to coastal communities in Alaska. As recent research demonstrates that limiting warming to 1.5 °C and even 2 °C is unlikely unless there is transformative global action to reduce carbon emissions [47], these estimates of ice loss may be conservative, further emphasizing the vulnerability of Alaskan coastal communities and the landfast ice environment.

Data availability statement

MODIS imagery is avaiable from NASA Earth Data (https://www.earthdata.nasa.gov/sensors/modis). ERA5 Climate Reanalysis Data is available from Copernicus (https://cds.climate.copernicus.eu/cdsapp#!/dataset/reanalysis-era5-single-levels). Bathymetry data are available from GEBCO (https://www.gebco.net/data_and_products/gridded_bathymetry_data/gebco_2022/). Drift ice concentration data is available from NSIDC (https://nsidc.org/data/g02135/versions/3).

The data that support the findings of this study are openly available at the following URL/DOI: https://doi.org/10.5281/zenodo.10413148.

References

[1] Eicken H, Lovecraft A L and Druckenmiller M L 2009 Sea-ice system services: a framework to help identify and meet information needs relevant for Arctic observing networks *Arctic* **62** 119–36
[2] Wang J, Mizobata K, Bai X, Hu H, Jin M, Yu Y, Ikeda M, Johnson W, Perie W and Fujisaki A 2014 A modeling study of coastal circulation and landfast ice in the nearshore Beaufort and Chukchi seas using CIOM *J. Geophys. Res. Oceans* **119** 3285–312
[3] Mahoney A, Eicken H, Gaylord A G and Shapiro L 2007 Alaska landfast sea ice: links with bathymetry and atmospheric circulation *J. Geophys. Res.* **112** C2
[4] Lantuit H and Pollard W H 2008 Fifty years of coastal erosion and retrogressive thaw slump activity on Herschel Island, southern Beaufort Sea, Yukon Territory, Canada *Geomorphology* **95** 84–102
[5] Overeem I, Anderson R S, Wobus C W, Clow G D, Urban F E and Matell N 2011 Sea ice loss enhances wave action at the Arctic coast *Geophys. Res. Lett.* **38** 1–6
[6] Hošeková L, Eidam E, Panteleev G, Rainville L, Rogers W E and Thomson J 2021 Landfast ice and coastal wave exposure in Northern Alaska *Geophys. Res. Lett.* **48** e2021GL095103
[7] Laidre K L, Stirling I, Lowry L, Wiig O, Heide-Jorgensen M P and Ferguson S H 2008 Quantifying the sensitivity of Arctic

marine mammals to climate-induced habitat change *Ecol. Appl.* **18** 97–125

[8] Gearheard S, Matumeak W, Angutikjuaq I, Maslanik J, Huntington H P, Gearheard S, Kagak D M, Tigullaraq G and Barry R G 2006 It's not that simple": a collaborative comparison of Sea ice environments, their uses, observed changes, and adaptations in barrow, Alaska, USA, and Clyde River, Nunavut, Canada *AMBIO: J. Hum. Environ.* **35** 203–11

[9] Druckenmiller M L, Eicken H, George J C and Brower L 2010 Assessing the shorefast ice: Iñupiat whaling trails off barrow, Alaska *SIKU: Knowing Our Ice* (Springer) pp 203–28

[10] Baztan J, Cordier M, Huctin J M and Zhu Z 2017 Life on thin ice: insights from Uummannaq, Greenland for connecting climate science with Arctic communities *Polar Sci.* **13** 100–8

[11] Hauser D D W *et al* 2021 Co-production of knowledge reveals loss of Indigenous hunting opportunities in the face of accelerating Arctic climate change *Environ. Res. Lett.* **16** 095003

[12] George J C C, Huntington H P, Brewster K, Eicken H, Norton D W and Glenn R 2004 Observations on shorefast ice dynamics in Arctic Alaska and the responses of the Iñupiat hunting community *Arctic* **57** 363–74

[13] Ford J D, Gough W A, Laidler G J, Macdonald J, Irngaut C and Qrunnut K 2009 Sea ice, climate change, and community vulnerability in northern Foxe Basin, Canada *Clim. Res.* **38** 137–54

[14] Meier W N, Stroeve J and Gearheard S 2006 Bridging perspectives from remote sensing and Inuit communities on changing sea-ice cover in the Baffin Bay region *Ann. Glaciol.* **44** 433–8

[15] Dammann D O, Eriksson L E B, Mahoney A R, Eicken H and Meyer F J 2019 Mapping pan-Arctic landfast sea ice stability using Sentinel-1 interferometry *Cryosphere* **13** 557–77

[16] Mahoney A R, Eicken H, Gaylord A G and Gens R 2014 Landfast sea ice extent in the Chukchi and Beaufort Seas: the annual cycle and decadal variability *Cold Reg. Sci. Technol.* **103** 41–56

[17] Yu Y, Stern H, Fowler C, Fetterer F and Maslanik J 2014 Interannual variability of Arctic landfast ice between 1976 and 2007 *J. Clim.* **27** 227–43

[18] Galley R J, Else B G T, Howell S E L, Lukovich J V and Barber D G 2012 Landfast Sea ice conditions in the Canadian Arctic: 1983–2009 *Arctic* **65** 133–44

[19] Howell S E L, Laliberté F, Kwok R, Derksen C and King J 2016 Landfast ice thickness in the Canadian Arctic Archipelago from observations and models *Cryosphere* **10** 1463–75

[20] Cooley S W, Ryan J C, Smith L C, Horvat C, Pearson B, Dale B and Lynch A H 2020 Coldest Canadian Arctic communities face greatest reductions in shorefast sea ice *Nat. Clim. Change* **10** 533–8

[21] Rantanen M, Karpechko A, Lipponen A, Nordling K, Hyvärinen O, Ruosteenoja K, Vihma T and Laaksonen A 2022 The Arctic has warmed nearly four times faster than the globe since 1979 *Commun. Earth Environ.* **3** 168

[22] Irrgang A M *et al* 2022 Drivers, dynamics and impacts of changing Arctic coasts *Nat. Rev. Earth Environ.* **3** 39–54

[23] Jones B M, Arp C D, Jorgenson M T, Hinkel K M, Schmutz J A and Flint P L 2009 Increase in the rate and uniformity of coastline erosion in Arctic Alaska *Geophys. Res. Lett.* **36** 3

[24] Liew M, Xiao M, Jones B M, Farquharson L M and Romanovsky V E 2020 Prevention and control measures for coastal erosion in northern high-latitude communities: a systematic review based on Alaskan case studies *Environ. Res. Lett.* **15** 093002

[25] Manson G K and Solomon S M 2007 Past and future forcing of Beaufort Sea coastal change *Atmosphere* **45** 107–22

[26] Farquharson L M, Mann D H, Swanson D K, Jones B M, Buzard R M and Jordan J W 2018 Temporal and spatial variability in coastline response to declining sea-ice in northwest Alaska *Mar. Geol.* **404** 71–83

[27] Lovvorn J R, Rocha A R, Mahoney A H and Jewett S C 2018 Sustaining ecological and subsistence functions in conservation areas: eider habitat and access by Native hunters along landfast ice *Environ. Conserv.* **45** 361–9

[28] Mahoney A R *et al* 2021 Thin ice, deep snow and surface flooding in Kotzebue Sound: landfast ice mass balance during two anomalously warm winters and implications for marine mammals and subsistence hunting *J. Glaciol.* **67** 1013–27

[29] US Census Bureau 2020 Alaska population estimates, 2020

[30] GEBCO Compilation Group 2022 GEBCO_2022 Grid (https://doi.org/10.5285/e0f0bb80-ab44-2739-e053-6c86abc0289c)

[31] Hersbach H *et al* 2020 The ERA5 global reanalysis *Q. J. R. Meteorol. Soc.* **146** 1999–2049

[32] Graham R M, Hudson S R and Maturilli M 2019 Improved performance of ERA5 in Arctic gateway relative to four global atmospheric reanalyses *Geophys. Res. Lett.* **46** 6138–47

[33] Fetterer F, Knowles K, Meier W H, Savoie M and Windnagel A K 2017 *Sea Ice Index, Version 3* (NSIDC: National Snow and Ice Data Center) (https://doi.org/10.7265/N5K072F8)

[34] Schober P, Boer C and Schwarte L A 2018 Correlation coefficients: appropriate use and interpretation *Anesth. Analg.* **126** 1763–8

[35] D'Agostino R and Pearson E S 1973 Tests for departure from normality. empirical results for the distributions of b 2 and √b 1 *Biometrika* **60** 613

[36] Mann H B 1945 Nonparametric tests against trend *Econometrica* **13** 245

[37] Hamed K H and Ramachandra Rao A 1998 A modified Mann-Kendall trend test for autocorrelated data *J. Hydrol.* **204** 182–96

[38] Hamed K H 2008 Trend detection in hydrologic data: the Mann–Kendall trend test under the scaling hypothesis *J. Hydrol.* **349** 350–63

[39] Nederhoff K, Erikson L, Engelstad A, Bieniek P and Kasper J 2022 The effect of changing sea ice on wave climate trends along Alaska's central Beaufort Sea coast *Cryosphere* **16** 1609–29

[40] Ford J D, Clark D, Pearce T, Berrang-Ford L, Copland L, Dawson J, New M and Harper S L 2019 Changing access to ice, land and water in Arctic communities *Nat. Clim. Change* **9** 335–9

[41] Inoue J, Enomoto T, Miyoshi T and Yamane S 2009 Impact of observations from Arctic drifting buoys on the reanalysis of surface fields *Geophys. Res. Lett.* **36** 8

[42] Frey K E, Moore G W K, Cooper L W and Grebmeier J M 2015 Divergent patterns of recent sea ice cover across the Bering, Chukchi, and Beaufort seas of the Pacific Arctic Region *Prog. Oceanogr.* **136** 32–49

[43] Stabeno P J, Kachel N B, Moore S E, Napp J M, Sigler M, Yamaguchi A and Zerbini A N 2012 Comparison of warm and cold years on the southeastern Bering Sea shelf and some implications for the ecosystem *Deep Sea Res.* II **65–70** 31–45

[44] Petrich C, Eicken H, Zhang J, Krieger J, Fukamachi Y and Ohshima K I 2012 Coastal landfast sea ice decay and breakup in northern Alaska: key processes and seasonal prediction *J. Geophys. Res.* **117** 1–19

[45] Bronen R and Chapin F S 2013 Adaptive governance and institutional strategies for climate-induced community relocations in Alaska *Proc. Natl Acad. Sci. USA* **110** 9320–5

[46] Ashjian C J *et al* 2010 Climate variability, oceanography, bowhead whale distribution, and Iñupiat subsistence whaling near barrow climate variability, oceanography, bowhead whale distribution, and inupiat subsistence whaling near Barrow, Alaska *Arctic* **63** 179–94

[47] Hoegh-Guldberg O *et al* 2019 The human imperative of stabilizing global climate change at 1.5 °C *Science* **365** eaaw6974